Chinese Chemical Letters 35 (2024) 109699

Contents lists available at ScienceDirect

Chinese Chemical Letters

journal homepage: www.elsevier.com/locate/cclet

Constructing bifunctional magnetic porous poly(divinylbenzene) polymer for high-efficient removal and sensitive detection of bisphenols

Mengyuan Li[a], Xitong Ren[b], Yanmei Gao[a], Mengyao Mu[a], Shiping Zhu[a], Shufang Tian[a], Minghua Lu[a,*]

[a] College of Chemistry and Molecular Sciences, Henan University, Kaifeng 475004, China
[b] Key Laboratory for Special Functional Materials of Ministry of Education, School of Materials Science and Engineering, Henan University, Kaifeng 475004, China

ARTICLE INFO

Article history:
Received 11 December 2023
Revised 14 February 2024
Accepted 27 February 2024
Available online 1 March 2024

Keywords:
Sample pretreatment
Bisphenols (BPs)
Porous organic polymer
Magnetic solid-phase extraction (MSPE)
Adsorption

ABSTRACT

In view of widespread existence and toxicity, removal and detection of bisphenols is imperative to assess environmental risks and reduce harm to human health. Although many techniques have been reported, constructing fast and sensitive method remains a challenge. Herein, porous poly(divinylbenzene) polymer was synthesized *in-situ* on the Fe_3O_4 particles by means of distillation-precipitation polymerization and functioned as sorbents to extract bisphenols. Employing Fe_3O_4@poly(divinylbenzene) as sorbent, a magnetic solid-phase extraction coupling with liquid chromatography was developed to detect trace bisphenols in water. This method presented low detection limits (0.01–0.03 ng/mL), high enrichment ability (enrichment factor, 327–343), and good reproducibility. Moreover, the method showed satisfactory recoveries in the detection of lake water (80.60%-116.2%) and egg sample (75.17%-120.0%). Impressively, Fe_3O_4@PDVB has excellent adsorption capacity, which can realize rapid kinetic adsorption of bisphenols with equilibrium time all less than 10 s. The maximum adsorption capacities reached 1074.8, 1049.7, 1299.1 and 1329.5 mg/g for bisphenol F, bisphenol A, bisphenol B and bisphenol AF with Langmuir isotherm model. The adsorption mechanism of Fe_3O_4@PDVB to bisphenols was investigated and demonstrated that hydrophobic interactions played a key role, together with assistance of $\pi-\pi$ stacking interactions and hydrogen interactions. Overall, this work provides a promising sorbent material with ultra-fast and large adsorption capacities for extraction of bisphenols from water.

As a significant monomer to prepare polycarbonates and epoxy resins, bisphenol A (BPA) are widely utilized in the manufacture of baby bottles, beverage packaging, dental sealants, and other products. Due to estrogen-like effects, BPA can cause biological reproductive abnormalities and disrupt normal endocrine functions in humans even at very low concentrations [1,2]. The overuse of BPA will cause various environmental pollution [3,4]. In recent years, bisphenol B (BPB), bisphenol F (BPF) and bisphenol AF (BPAF) were used as substitutes for BPA. However, more and more evidences demonstrate that they have equally harmful to species and ecosystems [5,6]. Therefore, it is very necessary to develop sensitive method for detection of trace bisphenols (BPs).

Owing to extremely low concentration in real samples and serious interferences from other coexisting matrices, a high-efficient sample pretreatment is usually required before separation and detection of BPs [7]. Due to can greatly improve recovery of sorbent materials and simplify procedures of sample pretreatment with combination of magnetic separation and solid-phase extraction, magnetic solid phase extraction (MSPE) received considerable attention [8–11]. As a key part of MSPE, the sorbents not only affect sensitivity and selectivity, but also influence reliability and accuracy of the analytical methods [12]. Therefore, various new materials such as carbon materials [13,14], covalent organic frameworks [15–17], metal-organic frameworks [18–21], porous polymers [22,23] and their functional composites were explored as sorbents in sample pretreatment.

Porous organic polymers with offering unprecedented structural features including tunable structures, diverse synthesis processes, versatility and extraordinary framework stability, have provided great opportunities for applications in energy storage [24], elemental capture [25], pollutants removal [26,27], photodegradation [28] as well as separation, sensing and drug delivery [29–31].

* Corresponding author.
E-mail address: mhlu@henu.edu.cn (M. Lu).

https://doi.org/10.1016/j.cclet.2024.109699
1001-8417/

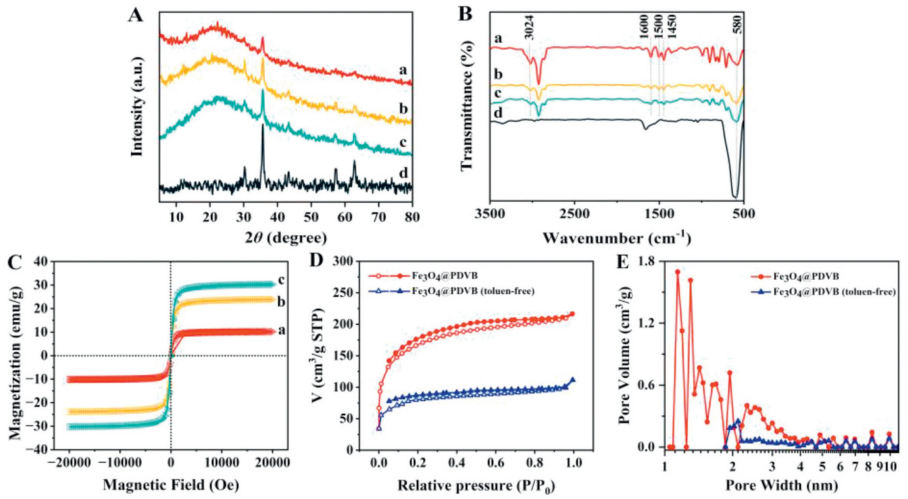

Fig. 1. XRD patterns (A), IR spectra (B), magnetic hysteresis loops (C), N_2 adsorption-desorption (D) and pore size distribution profile (E) of Fe_3O_4@PDVB. Spectra a, b, c and d represent 2.4%Fe_3O_4@PDVB, 7.3%Fe_3O_4@PDVB, 12.2%Fe_3O_4@PDVB and Fe_3O_4, respectively.

The plenty of pore structures and active sites make these materials to be considered as an ideal candidate for sample pretreatment [32]. Poly(divinylbenzene) (PDVB) as a highly cross-linked polymer has been demonstrated ideal sorbent for preconcentration of trace targets [33,34]. However, in the process of sample pretreatment, the retrieve of PDVB from sample solution has difficulty because of super-light property.

Herein, a series porous Fe_3O_4@PDVB polymers were prepared with *in-situ* self-polymerization strategy. The Fe_3O_4 particles are encapsulated inside the polymer to form magnetic PDVB. The phase separation and retrieve of sorbent can be easily performed with an external magnet, which overcomes the difficulty of separating PDVB from aqueous solution by centrifugal process because of its ultra-light nature in solution. The Fe_3O_4@PDVB nanoparticles were used as sorbent of MSPE to high-efficient extract four BPs (Table S1 in Supporting information) and sensitive detect them with high-performance liquid chromatography (HPLC) technique.

The Fe_3O_4@PDVB was characterized with X-ray diffraction (XRD) technique. As is shown in Fig. 1A, a broad peak appears at 10° to 30°, which is consistent with the previously reported peak of PDVB [35]. Spectrogram d in Fig. 1A is the XRD diffraction pattern of the prepared pure Fe_3O_4. The 220, 311, 400, 422, 511, 440 planes of spinel Fe_3O_4 and their diffraction peak relative intensities are in good accordance with the previous reported [36]. Similarly, these diffraction peaks can be found in Fe_3O_4@PDVB, and intensity of characteristic diffraction peak increases gradually with improving Fe_3O_4 content in the synthesis.

Infrared (IR) spectrum can provide significant information of functional groups and chemical bonds. Fig. 1B demonstrates the typical IR spectra of Fe_3O_4@PDVB. The absorption peak at 3024 cm^{-1} is ascribed to C–H stretching vibration of unsaturated carbon. Generally, C–H stretching of saturated hydrocarbons is below 3000 cm^{-1} and close to the frequency absorption of 3000 cm^{-1}. The peaks at 1600, 1500, 1450 cm^{-1} are attributed to stretching vibration of benzene ring skeleton, and peaks at 880–680 cm^{-1} belong to the C–H bending vibration of aromatic compound. The characteristic peaks of main functional groups in composite have been interpreted successfully.

As expected, the magnetic hysteresis loops in Fig. 1C show that the saturation magnetization increases with the increase of Fe_3O_4 content. The saturation magnetization strengths of the materials containing 2.4%Fe_3O_4@PDVB, 7.3%Fe_3O_4@PDVB, and 12.2%Fe_3O_4@PDVB were measured to be 11.0, 24.3, and 31.3 emu/g, respectively. All three hysteresis loops pass through the origin, indicating that all three substances are paramagnetic, which provide a prerequisite for their use in the MSPE process.

Contact angle test was used to determine the material's hydrophobicity. As presented in Fig. S1 (Supporting information), the apparent contact angles of Fe_3O_4@PDVB with three different Fe_3O_4 contents are all higher than 90°, which indicates that the surface of Fe_3O_4@PDVB is hydrophobic property.

The size of specific surface area is closely related to material size, shape, surface defects and pore structure. Stronger surface effects like surface activity and surface adsorption capacity are associated with greater specific surface areas. The N_2 adsorption-desorption isotherm of 7.3%Fe_3O_4@PDVB is displayed in Fig. 1D. The curve shows a rapid increase in adsorption at lower relative pressures, indicating a potent interaction between the material and N_2. Thereafter, a saturation value of adsorption occurs after reaching a certain relative pressure, similar to the Langmuir adsorption isotherm. These are typical features of type I isotherms. In general, type I isotherms tend to reflect the microporous filling phenomenon on microporous adsorption. Fig. 1E reflects the pore size distribution of 7.3%Fe_3O_4@PDVB, which verifies our previous analysis that a large amount of micropores exist in the material. These characterization results suggested that the sorbent possesses large surface area and high porosity. In addition, the 7.3%Fe_3O_4@PDVB without the addition of a pore-forming agent (toluene) during the synthesis process were also investigated. In Fig. 1D, the specific surface area of toluene-free Fe_3O_4@PDVB (268 m^2/g) with blue color was much lower than that of Fe_3O_4@PDVB (560 m^2/g) with red color. The average pore sizes of toluene-free Fe_3O_4@PDVB and Fe_3O_4@PDVB were 4.12 nm and 2.65 nm. It can be concluded that the microporous structure of material was greatly increased, and specific surface area of Fe_3O_4@PDVB improved after addition of toluene during the synthesis.

The morphological structures of the 7.3%Fe_3O_4@PDVB were characterized by SEM and TEM. It is evident from the SEM image (Figs. 2A and B) that the bar-like 7.3%Fe_3O_4@PDVB is staggered and the overall morphology resembles coral. The TEM images (Figs. 2C and D) bring out the structure of material more clearly. The bare Fe_3O_4 magnetic nanoparticles had assembled spherical morphology with an approximate size of 170 nm, and the PDVB layer surrounding the magnetic core could be distinctly observed. Furthermore, there are almost no residual pure PDVB polymers present in the 7.3%Fe_3O_4@PDVB sample. This phenomenon indicates that

Table 1
The linear range, R^2, LOD, LOQ, EFs and RSD of the MSPE using 7.3%Fe_3O_4@PDVB as sorbent for the analysis of BPs.

Analyte	Linear range (ng/mL)	R^2	LOD (ng/mL)	LOQ (ng/mL)	EF	RSD (%)	
						Intra-day (n = 5)	Inter-day (n = 5)
BPF	0.05–200	0.9973	0.02	0.05	327	3.45	7.43
BPA	0.03–200	0.9996	0.01	0.03	343	3.66	6.59
BPB	0.05–200	0.9984	0.02	0.05	327	3.26	6.67
BPAF	0.10–200	0.9993	0.03	0.10	334	3.65	5.95

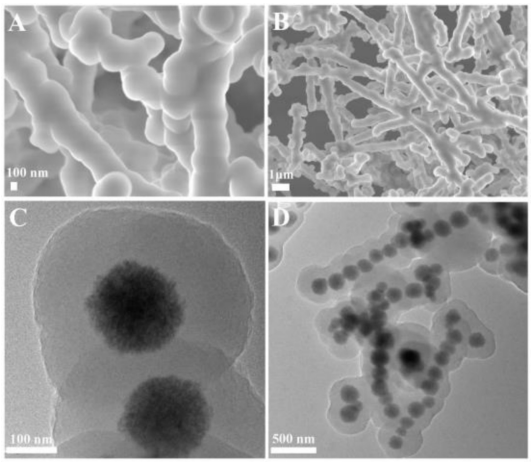

Fig. 2. SEM (A, B) TEM (C, D) images of 7.3%Fe_3O_4@PDVB.

the PDVB polymers have been entirely covered on the surfaces of Fe_3O_4 magnetic nanoparticles to form well-defined coating layers.

To achieve high extraction performance, the process of sample pretreatment was usually performed in different solvents or solution with different pH values. Therefore, the stability of 7.3%Fe_3O_4@PDVB in acidic (pH - 2), alkaline (pH - 10) and salt solution (1 mol/L NaCl) media were evaluated. After soaking for 24 h, XRD and IR spectrograms (Figs. S2A and B in Supporting information) demonstrated that the structure of the sample did not change. In addition, there was no obvious weight loss of 7.3%Fe_3O_4@PDVB within the temperature of 420 °C (Fig. S2C in Supporting information). This can be attributed to the fact that PDVB is a highly cross-linked carbon-carbon structure, and the Fe_3O_4 magnetic spheres also have high thermal stability.

The adsorption performance of Fe_3O_4@PDVB with different molar mass ratios of Fe_3O_4 to BPs was evaluated under the same conditions. The results demonstrate that 7.3%Fe_3O_4@PDVB possesses higher extraction performance and precision compared with 2.4%Fe_3O_4@PDVB and 12.2%Fe_3O_4@PDVB (Fig. S3 in Supporting information). The SPME procedures were optimized to achieve ideal adsorption and desorption conditions. The detailed discussion and results are presented in supplementary information (Fig. S4 in Supporting information).

The linear range, limit of detection (LOD), limit of quantification (LOQ), coefficient of determination (R^2), enhancement factor (EF) and relative standard deviation (RSD) were achieved to analyze the performance of method (Table 1). The method presented excellent linearity for target BPs ranging 0.03–200 ng/mL with R^2 not less than 0.9973. The LODs with S/N at 3 were achieved between 0.01–0.03 ng/mL. LOQs (S/N = 10) of method were 0.03–0.10 ng/mL. The enrichment factor (EF) defined as the slope of the linear curve of the standard solution after enrichment by the MSPE method divided by slope of linear curve of the unenriched standard solution. The EF values of 7.3%Fe_3O_4@PDVB for BPs ranged from 327 to 343, which were significantly higher than those of the other materials (Table S2 in Supporting information). The RSDs of intra-day and inter-day were determined as 3.26%−3.66% and 5.95%−7.43%, respectively, which shows that the established method has good reproducibility. Besides, reusability is the key indicator to evaluate sorbent, because it relates to whether the sorbent can be used in practical production. The sorbent can be quickly eluted by methanol solution for re-adsorption and displayed high reusability. Experimental results showed that the extraction efficiency has not significant reduction within six times (Fig. S5 in Supporting information).

Fig. 3A present the adsorption kinetics of different BPs. It is a very fast adsorption process, which almost instantaneously reached equilibrium (within 10 s). The adsorption process was investigated with *pseudo*-first-order (Fig. 3B) and *pseudo*-second-order (Fig. 3C) kinetic models. The experimental results demonstrated the adsorption conform to *pseudo*-second-order kinetic model. The rate constant (k), the coefficient of determination (R^2), the experimental and calculated q_e values for BPs adsorption onto sorbents are calculated and summarized in Table S3 (Supporting information). All the R^2 values for BPF, BPA, BPB, and BPAF using *pseudo*-second-order kinetic model are above 0.9998, which are higher than those of the *pseudo*-first-order kinetic model. Additionally, the calculated q_e values and experimental q_e values are extremely similar. Conversely, the q_e calculated by *pseudo*-first-order kinetic model is obviously smaller than actual adsorption capacity. Therefore, *pseudo*-second-order kinetic model is more proper to describe adsorption of BPs with 7.3%Fe_3O_4@PDVB, indicating chemical reaction plays a role in the rate-controlling step. Furthermore, *pseudo*-second-order model is suitable for reaction in presence of saturation sites [37]. Therefore, multiple adsorption mechanisms were existed in the adsorption process of Fe_3O_4@PDVB on BPs. The equilibrium adsorption capacity of Fe_3O_4@PDVB on BPs gradually enhanced with increasing BPs concentration (Fig. 3D). The Langmuir (Fig. 3E) and Freundlich (Fig. 3F) models were applied to fit equilibrium data, and results are listed in Table S4 (Supporting information). The Langmuir model is based on assumption that the adsorption is on a uniform surface, forming a single molecule adsorption layer with the same energy at all adsorption sites. The Freundlich isotherm is an empirical equation used to describe heterogeneous surfaces with different adsorption site energies.

For the adsorption of BPs by 7.3%Fe_3O_4@PDVB, a good fit was observed for both Langmuir and Freundlich models. Even though the partial R^2 of Freundlich are slightly larger than that of Langmuir, which demonstrates Fe_3O_4@PDVB to BPs are multilayer adsorption, which affected by chemical and physical adsorption processes [38]. However, the adsorption physics models used by Freundlich and Langmuir are essentially the same, which can be seen from their derivation process. The difference is only the number of active centers that a molecule can saturate. When n = 1, Freundlich becomes Langmuir. For this reason, some experimental data on the adsorption of single molecule layers tend to fit well with both adsorption isotherms. When the Freundlich index ($1/n$) < 1, it also indicates monolayer adsorption, which is due to the curve tends to saturate with increasing Ce, while the multilayer adsorption does not saturate. In addition, the discussion of the N_2 adsorption-desorption isotherm above leads to the conclusion that the adsorption process of Fe_3O_4@PDVB is more consistent with the Langmuir

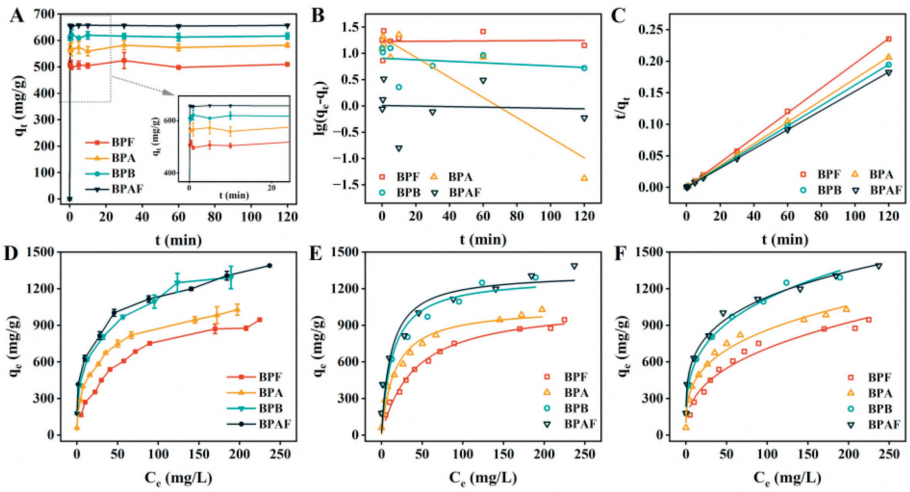

Fig. 3. Adsorption kinetics (A), *pseudo*-first-order (B), *pseudo*-second-order (C), adsorption isotherm (D), Langmuir model (E) and the Freundlich model (F) of BPs on the 7.3%Fe_3O_4@PDVB material.

model, that is, single molecular layer adsorption theory. Therefore, the Langmuir model was chosen here to calculate the theoretical adsorption amount (q_m), which proved that 7.3%Fe_3O_4@PDVB has a strong adsorption capacity. The monolayer saturation capacity, q_m, were determined as 1074.82, 1049.69, 1299.14, and 1329.48 mg/g for BPF, BPA, BPB, and BPAF, respectively.

Furthermore, the assumption of feasibility and nature of adsorption process were studied by R_L value. Details are listed as following: Irreversible ($R_L = 0$), indicating that the adsorption isothermal constant (a_L) is too large, which means that the adsorption force is too strong. Favorable ($0 < R_L < 1$), which is the standard case of normal adsorption. Linearity ($R_L = 1$) only occurs when $a_L = 0$, which means that adsorption isotherm is a straight line. Unfavorable ($R_L > 1$), which means $-1 < C_0 \times a_L < 0$, and instead of adsorption, which will have desorption. The obtained R_L values yielding between 0 and 1, indicating that the adsorption of Fe_3O_4@PDVB to BPs is a favorable process [39].

The adsorption process is often accompanied by the change of system energy. The adsorption thermodynamics are analyzed with the parameters of the change of Gibbs free energy (ΔG), enthalpy (ΔH), and entropy (ΔS). The detailed discussion and results are presented in supplementary information (Fig. S6 and Table S5 in Supporting information).

In order to fully understand the adsorption behavior of sorbent, the interactions between 7.3%Fe_3O_4@PDVB and BPs were investigated. According to their octanol-water partition coefficients ($\log K_{ow}$), the order of hydrophobicity is BPAF > BPB > BPA > BPF, which is basically in accordance with order of their q_m [40]. The phenyl and alkyl groups of BPs can produce hydrophobic interactions with 7.3%Fe_3O_4@PDVB. Compared with BPA, the fluoride groups of BPAF can further enhance the hydrophobicity. As a result, the adsorption capacity of 7.3%Fe_3O_4@PDVB to BPAF is higher than that of other analytes [41]. Therefore, the hydrophobic effect played a significant role during the adsorption. Moreover, π-π stacking interaction also can affect affinity of sorbents to targets [42]. Meanwhile, CH/π interactions, which are weak hydrogen bonds engendered between hydrogen atoms of alkyl or aryl group (H donor) and π-face of aromatic ring (H acceptor), also promotes adsorption [43,44]. In addition to the hydrophobic interactions, π-π stacking interactions and CH/π interactions as discussed above, 7.3%Fe_3O_4@PDVB also possessed rich internal pore environment and large specific surface area. As these plenty of pore structures that can facilitate exposure of internal absorbing sites to BPs and subsequently improve adsorption rate and capacity [26,45].

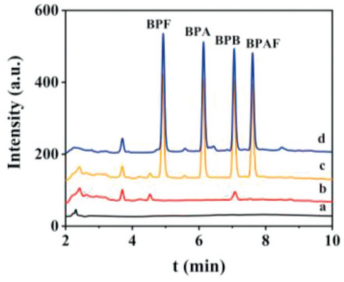

Fig. 4. The typical chromatograms obtained for direct analysis of lake sample (a), lake sample pretreated with 7.3%Fe_3O_4@PDVB as MSPE sorbent (b), spiked water sample (100 ng/mL) pretreated with developed MSPE procedures (c) and the standard solution with a concentration of 100 ng/mL (d). Extraction and desorption conditions: (1) sorbent amount: 7 mg, (2) extraction time: 1 min, (3) desorption solvent: MeOH, (4) desorption time: 3 min.

To investigate the ability of method to analyze real samples, the developed MSPE-HPLC method was applied to extraction and determination of BPs in Baogong Lake (Kaifeng, China). The specific detection process of this method is shown in Fig. S9 (Supporting information). Firstly, samples were analyzed without pretreatment, and result illustrated as chromatogram a in Fig. 4. It can be seen that no obvious peaks were observed. The chromatogram b in Fig. 4 shows a typical chromatogram for the analysis of water sample with developed method using 7.3%Fe_3O_4@PDVB as the sorbent of MSPE under optimal conditions. Preliminary analysis indicated that the sample contained a small amount of BPB, and the concentration was calculated as 6.45 ng/mL. Additionally, three different concentrations of BPs standard solutions (1, 10, and 100 ng/mL) were added to the actual samples and the accuracy was investigated with calculating their recoveries. The chromatograms c and d (Fig. 4) were obtained from determination of spiked water and standard solution using developed method. Recoveries ranged from 80.60% to 116.2% were achieved for analysis of lake water sample (Table S6 in Supporting information). The matrix effect which has great influence on quantification was also studied. All these results showed that the suppressive effects of lake water components on the BPs were in the range of 0.8 to 0.9, which belongs to mild suppression effect (Table S7 in Supporting information). The method

was also applied to analysis of egg sample. The results are presented in Table S8 (Supporting information). It can be seen that the recoveries for the analysis of egg sample were achieved between 75.17% to 120.0%.

The analytical parameters of developed MSPE-HPLC method were compared with other methods for analysis of BPs, and the data are listed in Tables S2 and S9 (Supporting information). As can be seen that the developed method presented a very short extraction time (within 10 s), which is much better than those of other reported methods. In addition, the maximum adsorption capacity of 7.3%Fe_3O_4@PDVB for BPs used in this experiment was much higher than that of other sorbents. Moreover, it exhibited lower LOD and higher enrichment factors in comparison with the works. In addition, we verified the adsorption selectivity of 7.3%Fe_3O_4@PDVB to different pollutants (Figs. S7 and S8 in Supporting information). The adsorption properties of sulfonamides, Pb(II) and dyes were tested. These results suggested that 7.3%Fe_3O_4@PDVB has some selectivity for BPs (Table S10 in Supporting information). Overall, the developed method owns cost-effective, saving time, high efficiency and high sensitivity, which can be used to analysis of BPs in water more effectively than other reported methods.

In this work, porous 7.3%Fe_3O_4@PDVB was produced by a facile method and used as a sorbent for MSPE to enrich BPs in water. The 7.3%Fe_3O_4@PDVB exhibited ultrafast adsorption rate and very large adsorption capacity for BPs. The equilibrium could be reached within 10 s. The adsorption capacities of Fe_3O_4@PDVB for BPF, BPA, BPB, and BPAF were 1074.8, 1049.7, 1299.1, and 1329.48 mg/g, respectively. The enrichment effect of porous 7.3%Fe_3O_4@PDVB on BPs is remarkable, which is far superior to the reported methods. Extensive experiments validated the reasonableness of the above analysis and the reliability of the constructed MSPE-HPLC method. All these advantages make porous 7.3%Fe_3O_4@PDVB as an ideal sorbent candidate for remove and extraction of BPs in real samples.

Declaration of competing interest

The authors declare that they have no known competing financial interests or personal relationships that could have appeared to influence the work reported in this paper.

Acknowledgments

This work was sponsored by the National Natural Science Foundation of China (Nos. 22076038 and 22376053), and Henan key scientific research programs to Universities and Colleges (No. 22ZX003).

Supplementary materials

Supplementary material associated with this article can be found, in the online version, at doi:10.1016/j.cclet.2024.109699.

References

[1] Y. Ma, H. Liu, J. Wu, et al., Environ. Res. 176 (2019) 108575.
[2] P. Qin, S. Zhu, M. Li, et al., Chin. Chem. Lett. 34 (2023) 108620.
[3] J. Liu, L. Zhang, G. Lu, et al., Environ. Saf. 208 (2021) 111481.
[4] A. Tarafdar, R. Sirohi, P.A. Balakumaran, et al., J. Hazard. Mater. 423 (2022) 127097.
[5] Z. Gao, S. Liu, L. Tan, et al., Sci. Total Environ. 836 (2022) 155628.
[6] F. Navarro-Lafuente, E. Adoamnei, J.J. Arense-Gonzalo, et al., Sci. Total Environ. 838 (2022) 156540.
[7] L. Han, X. Liu, X. Zhang, et al., J. Hazard. Mater. 424 (2022) 127559.
[8] B. Zhao, W. Xu, J. Ma, Q. Jia, Chin. Chem. Lett. 34 (2023) 107498.
[9] Y. Gao, S. Zhu, M. Mu, et al., Chem. Eng. J. 475 (2023) 146459.
[10] L. Qiao, C. Yu, R. Sun, J. Anal. Test. 6 (2022) 401–410.
[11] A.K. El-Deen, C.M. Hussain, Trends Environ. Anal. Chem. 39 (2023) e00211.
[12] X. Zhang, Y. Yang, P. Qin, al. et, Chin. Chem. Lett. 33 (2022) 903–906.
[13] Z. Zhao, B. Liang, M. Wamg, et al., Chem. Eng. J. 427 (2022) 130943.
[14] T. Lu, Q. Wang, J. Kong, al. et, Chem. Eng. J. 448 (2022) 137690.
[15] J. Cheng, J. Ma, S. Li, et al., J. Hazard. Mater. 461 (2024) 132613.
[16] W. Ma, Q. Zheng, Y. He, et al., J. Am. Chem. Soc. 141 (2019) 18271–18277.
[17] X. Yan, Y. Yang, G. Li, et al., Chin. Chem. Lett. 34 (2023) 107201.
[18] L. Han, P. Qin, M. Li, et al., Chem. Eng. J. 456 (2023) 140969.
[19] P. Qin, D. Chen, D. Li, et al., Food Chem. 409 (2023) 135272.
[20] Y. Wu, H. Chen, Y. Chen, et al., Sci. China Chem. 65 (2022) 650–677.
[21] X. Zhang, Y. Zhang, W. Zhou, et al., Chin. Chem. Lett. 34 (2023) 107368.
[22] S. Qin, S. Qi, X. Li, et al., Sci. Total Environ. 728 (2020) 138789.
[23] B. Zhao, L. Jiang, Q. Jia, Chin. Chem. Lett. 33 (2022) 11–21.
[24] L. Xiang, S. Yuan, F. Wang, et al., J. Am. Chem. Soc. 144 (2022) 15497–15508.
[25] D. Chen, D. Luo, Y. He, et al., J. Am. Chem. Soc. 144 (2022) 16755–16760.
[26] A. Alsbaiee, B.J. Smith, L. Xiao, et al., Nature 529 (2016) 190–U146.
[27] X. Liu, C. Zhu, J. Yin, et al., Nat. Commun. 13 (2022) 2132.
[28] R. Hu, M. Hassan, S. Zhang, W. Gong, Chin. Chem. Lett. 34 (2023) 107541.
[29] Z. Li, Y. Yang, Adv. Mater. 34 (2022) 2107401.
[30] H. Sai, K.W. Tan, K. Hur, Science 341 (2013) 530–534.
[31] Y. Zhu, P. Xu, X. Zhang, et al., Chem. Soc. Rev. 51 (2022) 1377–1414.
[32] S. Jiang, Z. Li, X. Yang, et al., Food Chem. 404 (2023) 134652.
[33] M. Li, X. Ren, Y. Gao, et al., Chem. Commun. 58 (2022) 7574–7577.
[34] S.R. Churipard, K.S. Kanakikodi, D.A. Rambhia, et al., Chem. Eng. J. 380 (2020) 122481.
[35] Y. Zhang, S. Wei, W. Zhang, et al., ChemSusChem 2 (2009) 867–872.
[36] J. Liu, Z. Sun, Y. Deng, et al., Angew. Chem. Int. Ed. 48 (2009) 5875–5879.
[37] Y.S. Ho, G. McKay, Process Biochem. 34 (1999) 451–465.
[38] P. Wu, Z. Cai, H. Jin, et al., Sci. Total Environ. 650 (2019) 671–678.
[39] A. Kubiak, M. Mackiewicz, M. Biesaga, et al., J. Environ. Chem. Eng. 9 (2021) 104947.
[40] P. Lu, J. Cheng, Y. Li, et al., Carbohydr. Polym. 216 (2019) 149–156.
[41] Y. Feng, M. Sun, M. Sun, et al., J. Chromatogr. A 1673 (2022) 463132.
[42] L. Han, X. Zhang, D. Li, et al., Talanta 235 (2021) 122818.
[43] Y. Umezawa, S. Tsuboyama, H. Takahashi, et al., Carbohydr. Polym. 55 (1999) 10047–10056.
[44] T. Yamate, K. Kumazawa, H. Suzuki, et al., ACS Macro Lett. 5 (2016) 858–861.
[45] D. Schneider, D. Mehlhorn, P. Zeigermann, et al., Chem. Soc. Rev. 45 (2016) 3439–3467.